Laser Chem., 1995, Vol. 16, pp. 121–138
Reprints available directly from the publisher
Photocopying permitted by license only

© 1995 Harwood Academic Publishers GmbH
Printed in Malaysia

TIME-RESOLVED INVESTIGATION OF THE MOLECULAR CHEMILUMINESCENCE SrI($A^2\Pi_{1/2,3,2}$, $B^2\Sigma^+ \rightarrow X^2\Sigma^+$) AND THE ATOMIC RESONANCE FLUORESCENCE Sr($5^3P_1 \rightarrow 5^1S_0$) FOLLOWING THE PULSED DYE LASER GENERATION OF Sr(5^3P_J) IN THE PRESENCE OF CF_3I

S. ANTROBUS, D. HUSAIN* and JIE LEI,
Department of Chemistry, University of Cambridge, Lensfield Road, Cambridge CB2 IEW, England

F. CASTAÑO* and M.N. SANCHEZ RAYO,
Departamento de Quimica Fisica, Universidad del Pais Vasco, Apartado 644, 48080 Bilbao, Spain

(Received 11 February 1995)

A time-resolved investigation is presented of the electronic energy distribution in SrI following the collision of the optically metastable strontium atom, Sr [5s5p(^3P_J)], with the molecule CF_3I. Sr[5s5p(^3P_J)], 1.807 eV above its $5s^2(^1S_0)$ electronic ground state, was generated by pulsed dye-laser excitation of ground state strontium vapour to the Sr(5^3P_1) state at $\lambda = 689.3$ nm {Sr($5^3P_1 \leftarrow 5^1S_0$)} at elevated temperature (840 K) in the presence of excess helium buffer gas in which rapid Boltzmann equilibration within the 5^3P_J spin-orbit manifold takes place. Time resolved atomic emission from Sr($5^3P_1 \rightarrow 5^1S_0$) at the resonance transition and the molecular chemiluminescence from SrI($A^2\Pi_{1,2,3/2}$,$B^2\Sigma^+ \rightarrow X^2\Sigma^+$) resulting from reaction of the excited atom with CF_3I were recorded and shown to be exponential in character. SrI in the $A^2\Pi_{1/2,3/2}$ (172.5, 175.4 kJ mol^{-1}) and $B^2\Sigma^+$ (177.3 kJ mol^{-1}) states are energetically accessible on collision by direct-I-atomic abstraction between Sr(^3P) and CF_3I. The first-order decay coefficients for the atomic and molecular emissions are found to be equal under identical conditions and hence SrI($A^2\Pi_{1/2,3/2}$, $B^2\Sigma^+$) are shown to arise from direct I- atom abstraction reactions. The molecular systems recorded were SrI ($A^2\Pi_{1/2} \rightarrow X^2\Sigma^+$, $\Delta v = 0$, $\lambda = 694$ nm), SrI($A^2\Pi_{3/2} \rightarrow X^2\Sigma^+$, $\Delta v = 0$, $\lambda = 677$ nm) and SrI($B^2\Sigma^+ \rightarrow X^2\Sigma^+$) ($\Delta v = 0$, $\lambda = 674$ nm), dominated by the $\Delta v = 0$ sequences on account of Franck-Condon considerations. The combination of integrated molecular and atomic intensity measurements yields estimates of the branching ratios into the specific electronic states, $A_{1/2}$, $A_{3/2}$ and B, arising from Sr(5^3P_J)+CF_3I which are found to be as follows: $A_{1/2}$, 1.2×10^{-2}; $A_{3/2}$, 6.7×10^{-3}; B, 5.1×10^{-3} yielding $\Sigma SrI(A_{1/2}+A_{3/2}+B) = 2.4 \times 10^{-2}$. As only the X, A and B states SrI are accessible on reaction, assuming that the removal of Sr(5^3P_J) occurs totally by chemical removal, this yields an upper limit for the branching ratio into the ground state of ca. 98%. The present results are compared with previous time-resolved measurements on excited states of strontium halides that we have reported on various halogenated species resulting from reactions of Sr(5^3P_J), together with analogous chemiluminescence studies on Sr(^3P_J) and Ca(4^3P_J) from molecular beam measurements.

KEY WORDS: SrI Molecular Chemiluminescence, Laser Excitation, Electronically Excited Sr, Atomic Resonance Fluorescence.

*Authors to whom correspondence should be addressed.

INTRODUCTION

The combination of time-resolved atomic resonance fluorescence and time-resolved molecular chemiluminescence following pulsed dye-laser excitation has recently been developed to investigate electronic energy distribution in diatomic products following the collision of the low lying, optically metastable, strontium atom $Sr(5^3P_J)$, 1.807 eV above the $5s^2(^1S_0)$ ground state[1] with various mono-halide reactants.[2-5] Such studies are complementary to related measurements on this metastable atom in molecular beams,[6-8] a topic that has been reviewed in some detail especially in terms of the specific role of spin-orbit states within $Sr(5^3P_{0,1,2})$ by Campbell and Dagdigian,[9] and is of broad fundamental interest from the viewpoint of atomic collisions of electronically excited metal atoms in general.[10-13] Laser-induced fluorescence has also been employed to determine the energy distribution in the diatomic products of the reaction of $Sr(5^3P_J)$ with hydrogen halides and halogenated methanes under single collision conditions.[14,15] The time-resolved measurements on $Sr(5^3P_J)$ follow an earlier series of analogous investigations on the lighter calcium atom, $Ca[4s4p(^3P_J)]$.[16-19] The present paper extends the measurements of I-atom abstraction, in particular, by collisions of $Sr(5^3P_J)$, generated by pulsed dye-laser generation, using time-resolved atomic fluorescence and time-resolved molecular chemiluminescence from $SrI(A^2\Pi_{1/2,3/2,}B^2\Sigma^+ - X^2\Sigma^+)$. This type of investigation for SrI had hitherto proved technically difficult until very recently on account of the overlap between the relatively strong emission from higher lying states of Sr arising from 'energy pooling' from $Sr(5^3P_J)+Sr(5^3P_J)$ and the SrI(A,B-X) emissions. Energy pooling is a significant area in itself and is limited in this paper to those specific experimental aspects of the measurements that need to be considered when monitoring the relatively weak molecular emission from SrI(A,B-X) arising from the low branching ratios into the A and B states chemiluminescence which is monitored in the time-domain.[5] The time-dependent nature of the atomic and molecular emission measurements indicate that $SrI(A^2\Pi_{1/2,3/2,}B^2\Sigma^+)$ arises from direct reaction and can thus be related to analogous studies on the energy distribution in molecular beams. Integrated molecular and atomic intensities coupled with calibration of the optical system have further yielded estimates of branching ratios into the $A_{1/2}$, $A_{3/2}$, B and X states which are of a similar magnitude for analogous data obtained from various measurements on diatomic strontium halides (A,B,X) in the time-domain.[4,5,20,21] The total branching ratio into all the states $SrI(A_{1/2,3/2,}B)$ is, further, comparable with analogous data observed for halogen abstraction reactions by $Ca(4^3P_J)$ in molecular beams.[22] As we have stressed hitherto,[4,5,21,22] quantitative characterisation of branching ratios into specific electronic states from time-resolved measurements of the type described in this paper, in contrast to the measurements of total branching ratio into all excited states, constitutes a new development and is of fundamental interest.

EXPERIMENTAL

The experimental arrangement for generating $Sr(5^3P_J)$ and for monitoring atomic resonance fluorescence and molecular chemiluminescence in the time-domain was similar to that described in our recent investigations.[4,5,20,21] $Sr[5s5p(^3P_1)]$ was generated by pulsed dye-laser excitation (10 Hz) of strontium vapour at elevated temperatures[23]

(T = 840 K) at λ = 698.3 nm {Sr[5s5p($^3P_1$)] ←Sr[5s^2($^1S_0$)]} in the presence of CF_3I and excess helium buffer gas. A slow flow system, kinetically equivalent to a static system, at a constant flow rate, was employed. Measurements were carried out mainly at total pressures with He of 30 Torr and also 60 and 90 Torr (1 Torr = 133.3 Nm^{-2}) and integrated intensities recorded for all the atomic and molecular emission profiles, noting that calibration of the integrated intensities for the atomic emission profiles are required particularly in the analysis for determining the branching ratios into the $A_{1/2,3/2}$ and B states (see later), further noting that these ratios are not dependent on total pressure. Chemiluminescence from the systems SrI($A^2\Pi$,$B^2\Sigma^+ \rightarrow X^2\Sigma^+$)[24-27] and atomic emission at the resonance wavelength were then monitored under identical chemical conditions. Complete profiles for the atomic and molecular emissions were recorded for each individual decay. These were captured with a two-channel transient digitiser ('Digital Storage Adapter', Thurlby DSA 524) interfaced to a computer. 255 decay profiles were averaged as were 255 background profiles before transfer and subtraction for computerised analysis. All materials (Sr, He, CF_3I) were employed essentially as described in previous investigations.[4,5,19-21]

Measurements were made using different photomultiplier voltages for the atomic and molecular profiles on account of the small branching ratios into the excited molecular states and the subsequent weak emission and, of course, involving monitoring at different wavelengths. The molecular profiles are thus recorded at p.m. voltages considerably higher than those of the atomic emission. The gain (G) for the p.m. tube (E.M.I., 9797B, S20 response) can sensibly be fitted to the form ln (G/arb. units) = 8.7ln(V/Volts) − 54.4.[28] The wavelength response of the photomultiplier – grating combination using the 'Minichrom' monochromator (MC1-02-10288, Fastie-Ebert mounting; f/4; focal length 74 mm; range 200–800 nm; grating 20 mm square; 1800 lines per mm) was also calibrated. This employed a quartz-halogen lamp which had previously been calibrated against a spectral radiometer (International Light Inc., U.S.A. IL783). This yielded two maxima in the overall sensitivity response curve, one at ca. 440 nm and the other at ca. 510 nm, representing the expected effects of the combination of the blaze of the grating for the former and the maximum of the photomultiplier tube response for the latter. As we have stressed hitherto in general for these studies on Sr(5^3P_J),[4,5,20,21] a comparison of time-dependent profiles does not require the sensitivity calibrations. They are, however, required for the purposes of determining branching ratios into the specific electronic states where the atomic and molecular emission intensities need to be placed on a common relative scale.

RESULTS AND DISCUSSION

3.1. Time-Resolved Atomic and Molecular Chemiluminescence Measurements

Figure 1 shows examples of the digitized photoelectric output indicating the exponential decay of the time-resolved atomic emission from Sr(5^3P_1) at λ = 689.3 nm {Sr[5s5p($^3P_1$)] → Sr[5s^2($^1S_0$)]} following pulsed dye-laser excitation of strontium vapour at T = 840 K in the presence of varying concentrations of CF_3I and excess helium buffer gas and Figure 2, the associated computerised first-order decay profiles. In the presence of He alone, the appropriate first-order decay coefficients derived from

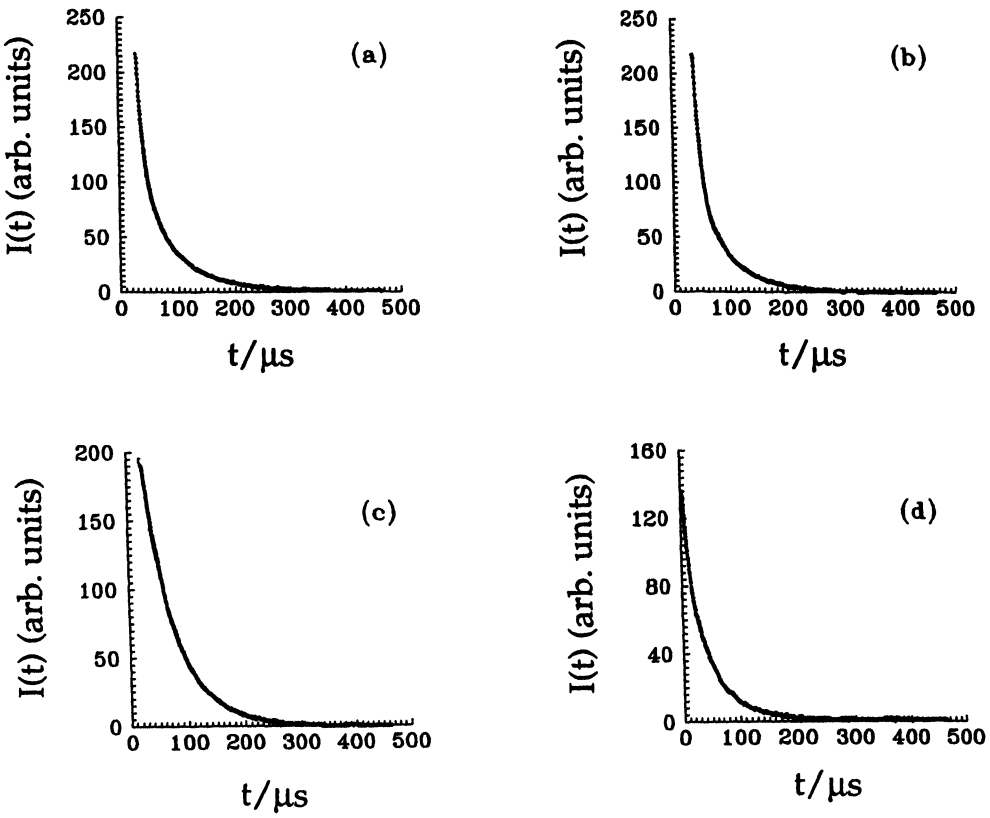

Figure 1 Examples of the digitized output indicating the exponential decay profiles for the time-resolved atomic fluorescence emission from $Sr(5^3P_1)$ at $\lambda = 689.3$ nm ($Sr(5^3P_1) \rightarrow Sr(5^1S_0)+h\nu$) following the pulsed dye-laser excitation of strontium vapour at the resonance wavelength in the presence of CF_3I and excess helium buffer gas at elevated temperature. ($T = 840$ K, $p_{\text{Total with He}} = 30$ Torr $- 3.9 \times 10^{17}$ atoms cm^{-3}) $[CF_3I]/10^{16}$ molecules cm^{-3}: (a) 0.95; (b) 1.2; (c) 1.4; (d) 1.8

the slopes of these plots may be expressed in the standard form:[29-31]

$$k' = A_{nm}/F + \beta/p_{He} \qquad \text{(i)}$$

where

$$F = 1 + 1/K_1 + K_2 \qquad \text{(ii)}$$

K_1 and K_2 represent the equilibrium constants connecting the spin-orbit states within $Sr(5^3P_J)$ ($^3P_0 \rightleftharpoons {}^3P_1, K_1; {}^3P_1 \rightleftharpoons {}^3P_2, K_2$) which rapidly reach Boltzmann equilibrium on the time-scales of the present measurements.[29,30] Emission is observed only from $Sr(5^3P_1)$,[30] and the term, β/p_{He}, represents the kinetic contribution to diffusional loss of $Sr(5^3P_J)$ which is small by comparison with spontaneous emission. The $5s5p(^3P_{0,2})$ spin-orbit states within $Sr(5^3P_J)$ are so called 'reservoir states' and emission from them can be neglected,[12,32] lengthening the effective radiative lifetime of $Sr(5^3P_1)$. The mean radiative lifetime of $Sr[5s5p(^3P_1)]$ has been well characterised by various methods (τ_e, $Sr(5^3P_1) \rightarrow Sr(5^1S_0) + h\nu(\lambda = 689.3$ nm): 19.6 μs,[29,30] 22 ± 0.5 μs[33]). The function F takes the value of 2.307 at $T = 840$ K, for example, and reaches a limiting value of 3

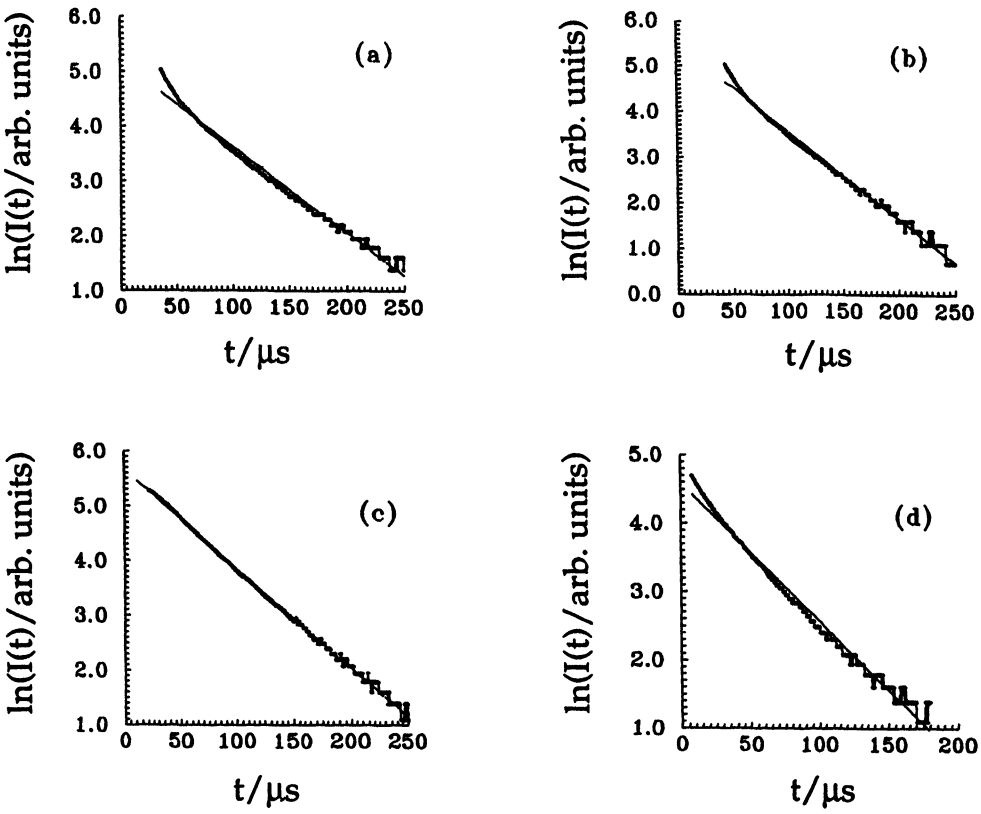

Figure 2 Examples of the computerized fitting of the digitized output indicating the first-order decay for the time-resolved atomic fluorescence emission from $Sr(5^3P_1)$ at $\lambda = 689.3$ nm ($Sr(5^3P_1) \rightarrow Sr(5^15_0)+h\nu$) following the pulsed dye-laser excitation of strontium vapour at the resonance wavelength in the presence of CF_3I and excess helium buffer gas at elevated temperature. ($T = 840$ K, $p_{Total\ with\ He} = 30$ Torr -3.9×10^{17} atoms cm^{-3}) $[CF_3I]/10^{16}$ molecules cm^{-3}: (a) 0.95; (b) 1.2; (c) 1.4; (d) 1.8

at infinite temperature, being determined solely by statistical weights with $Sr(5^3P_J)$. Although the detailed time scale by which the Boltzmann equilibrium has been reached for $Sr(5^3P_J)$ in helium alone is a matter of some controversy,[29,30,33] establishment of this equilibrium is rapid, as with $Ca(4^3P_J)$,[34,35] and the resulting mean radiative lifetimes, τ_e, for $Sr(5^3P_1)$ indicated above are not largely different for the various investigations and will not significantly affect the analysis in that regard in the present paper. Rapid spin-orbit relaxation within $Sr(5^3P_J)$ will be facilitated by CF_3I itself in these measurements.

In the presence of CF_3I, the first-order decay coefficients are given by the expression:

$$k' = A_{nm}/F + \beta/p_{He} + k_R[CF_3I] \qquad \text{(iii)}$$

where k_R is the overall absolute second-order rate constant for the removal of $Sr(5^3P_J)$ with CF_3I and where we could write

$$k' = K + k_R[CF_3I] \qquad \text{(iv)}$$

for constant total pressure and fixed temperature. The small variation in diffusional loss of $Sr(5^3P_J)$ indicated by the term β/p_{He} across the range 30–90 Torr (experimental) is negligible in comparison with other kinetic effects.[29,30] Figure 3 shows the variation of k′ with $[CF_3I]$ (initial) but this cannot be used to determine an accurate rate constant for the reaction of $Sr(5^3P_J)$ with CF_3I on account of the loss of CF_3I by reaction of this species with ground state $Sr(5^1S_0)$ before entry into the optical excitation region of the reactor. Clay and Husain[36,37] have reported absolute rate data for reactions of $Ca(4^1S_0)$ with various halides and where reaction efficiencies of *ca.* one in ten collisions were typically observed in the present temperature regime. We assume a similar reactivity for $Sr(5^1S_0)$, reducing the concentrations of CF_3I and yielding a scattered plot for Figure 3. The principal requirement in the present context for characterising the mechanism of reaction is that of identical conditions for comparing first-order decay coefficients for the atomic and molecular emissions at a given initial concentration. For estimating branching ratios into the $A^2\Pi_{1/2}$, $A^2\Pi_{3/2}$ and $B^2\Sigma^+$ states of SrI, and also an upper limit for the $X^2\Sigma^+$ state, the monotonic variation of k′ with $[CF_3I]$ is the principal requirement where we could use a term of the type $k_R f[CF_3I]$ in equations (iii) and (iv), where f is the fraction of the initial concentration of CF_3I reaching the laser optical excitation zone.

The profiles of the digitized output for the chemiluminescence from $SrI(A^2\Pi_{1/2} \rightarrow X^2\Sigma^+)$ at $\lambda = 694$ nm under identical conditions to those given in Figure 1 are given in Figure 4. Figure 5 shows the appropriate first-order plots yielding the molecular first-order decay coefficients for $Sr(A^2\Pi_{1/2})$. Analogous plots are given in Figures

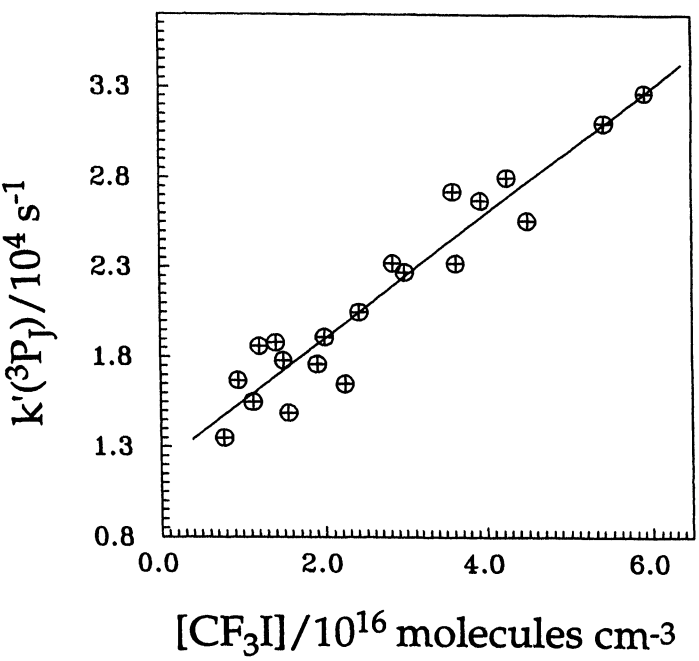

Figure 3 Variation of the pseudo first-order rate coefficients, $k'(^3P_J)$, for the decay of $Sr(5^3P_J)$, generated by pulsed dye-laser excitation at $\lambda = 689.3$ nm ($Sr(5^3P_1) \leftarrow Sr(5^1S_0)$) and monitored by time-resolved atomic fluorescence at the resonance wavelength in the presence of varying concentrations of CF_3I and excess helium buffer gas at T = 840 K.

6 and 7 for the chemiluminescence arising from the close lying $A^2\Pi_{3/2}$ state.[24,25] Molecular chemiluminescence measurements for SrI are essentially restricted to the $\Delta v = 0$ sequences for both the A-X and B-X systems. The Franck-Condon factors have been calculated using a modification of the programme for a Morse oscillator described by Tuckett [38,39] using the following parameters as hitherto:[5] $X^2\Sigma^+$ $\omega_e'' = 173.769$ cm^{-1}, $\omega_e''x_e'' = 0.3513$ cm^{-1}, $r_e'' = 0.2974$ nm; $A^2\Pi$ $\omega_e' = 181.0$ cm^{-1}, $\omega_e'x_e' = 0.35$ cm^{-1}, $r_e' = 0.2953$ nm; $B^2\Sigma^+$ $\omega_e' = 182.2$ cm^{-1}, $\omega_e'x_e' = 0.370$ cm^{-1} and $r_e' = 0.2944$ nm.[21-27,39]. Calculated Franck-Condon factors chosen here are restricted for the sequences $\Delta v = 0$ and ± 1 and to the vibrational levels $v = 0$ and 1 in the X, A and B states. Thus, we obtain for the A-X transition the following values: (0,0) 0.9432, (1,0) 5.505×10^{-2}, (1,1) 0.8340 and (0,1) 5.5390×10^{-2}. For the B-X transition, the analogous data are (0,0) 0.8857, (1,0) 0.1083, (1,1) 0.6835 and (0,1) 0.1066. Figure 8 shows examples of the SrI($B^2\Sigma^+ - X\Sigma^+$) digitized output for the molecular emission at $\lambda = 674$ nm ($\Delta v = 0$) following the pulsed dye-laser generation of Sr(5^3P_J) in the

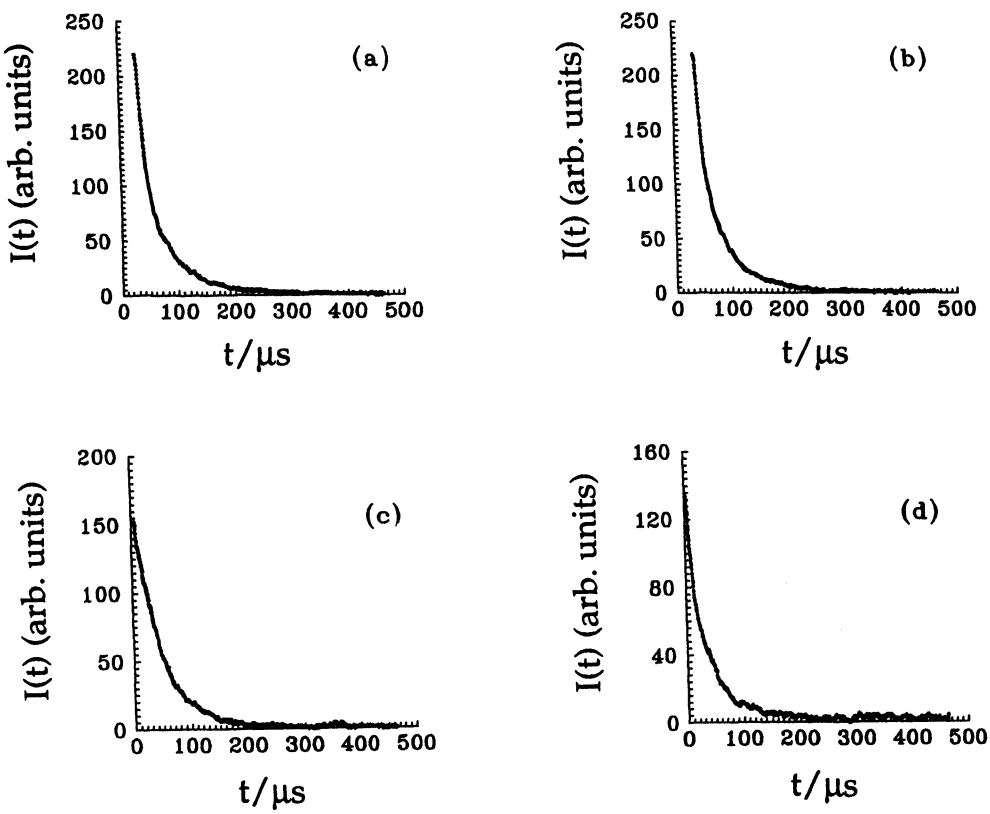

Figure 4 Examples of the digitized output indicating the exponential decay profiles for the time-resolved molecular chemiluminescence from SrI($A^2\Pi_{1/2} \rightarrow X^2\Sigma^+$) ($\lambda = 694$ nm, ($\Delta v = 0$)) following the pulsed dye-laser excitation of strontium vapour at $\lambda = 689.3$ nm (Sr(5^3P_1)) $\leftarrow$ Sr(5^1S_0)) in the presence of varying concentrations of CF_3I and excess helium buffer gas at elevated temperature. $T = 840$K $p_{\text{total with He}} = 30$ Torr $- 3.9 \times 10^{17}$ atoms cm^{-3} [CF_3I]/10^{16} molecules cm^{-3}): (a) 0.95; (b) 1.2; (c) 1.4; (d) 1.8

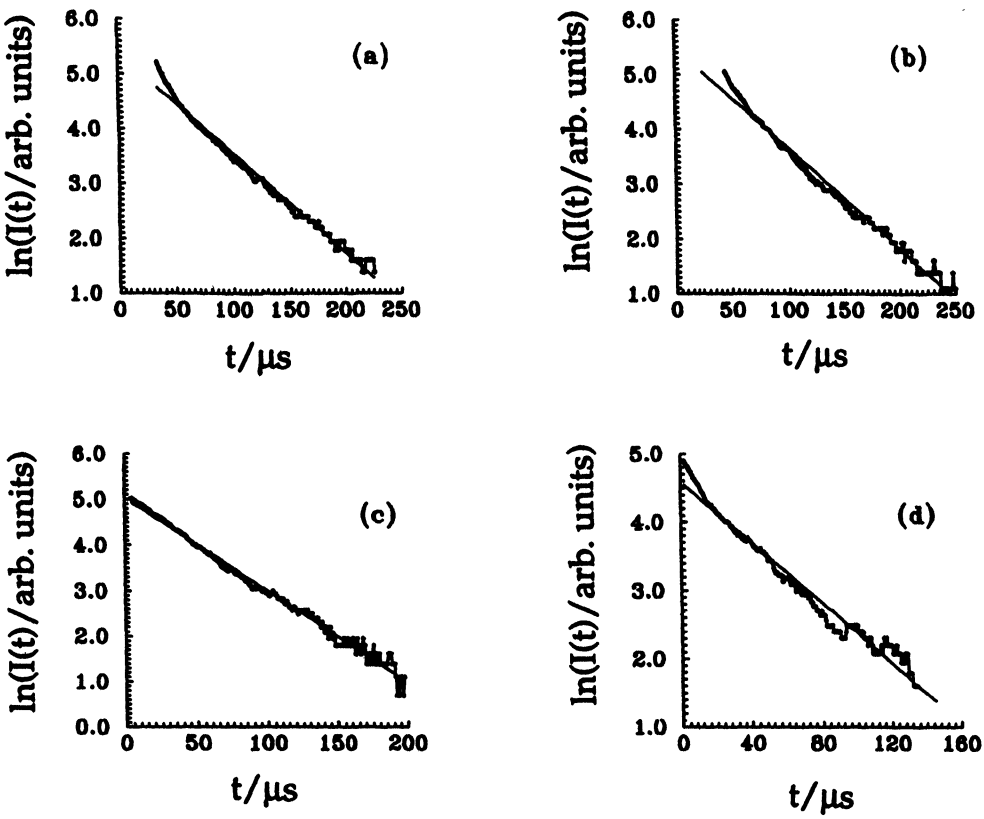

Figure 5 Examples of the computerised fitting of the digitized output indicating the first-order decay for the time-resolved molecular chemiluminescence from $SrI(A^2\Pi_{1/2} \rightarrow X^2\Sigma+)$ ($\lambda = 694$ nm, $(\Delta v = 0)$) following the pulsed dye-laser excitation of strontium vapour at $\lambda = 689.3$ nm ($Sr(5^3P_1) \leftarrow Sr(5^1S_0)$) in the presence of varying concentrations of CF_3I and excess helium buffer gas at elevated temperature. ($T = 840$K, $p_{Total\ with\ He} = 30$ Torr -3.9×10^{17} atoms cm^{-3}) $[CF_3I]/10^{16}$ molecules cm^{-3}: (a) 0.95; (b) 1.2; (c) 1.4; (d) 1.8

presence of varying concentrations of CF_3I taken under identical conditions to those described above with the resulting first-order plots shown in Figure 9.

Figures 10 shows the correlation between the measured first-order decays for the $A_{1/2,3/2}$–X and B-X emissions with those for the atomic emissions taken under identical conditions. The slopes of Figure 10(a) – (c) are found to be 1.04,1.06 and 1.04, respectively, unity in each case within experimental error. The 1σ errors are considered to be ca. 10% as the plots are placed through the origin which is a physically realistic point. It may thus be concluded that the atomic and molecular decay profiles are exponential in character and that the first-order decay coefficients are equal.

The thermochemistry for reaction between $Sr(5^3P_J)+CF_3I$ indicates that the $A^2\Pi_{1/2}$, $A^2\Pi_{3/2}$ and $B^2\Sigma^+$ states of SrI are clearly energetically accessible on collision:

$$Sr(5^3P_J)+CF_3I \rightarrow SrI(X^2\Sigma^+) + CF_3 \qquad \Delta H = -225.6 \text{ kJ mol}^{-1} \quad (1)$$

$$Sr(5^3P_J)+CF_3I \rightarrow SrI(A^2\Pi_{1/2}) + CF_3 \qquad \Delta H = -53.1 \text{ kJ mol}^{-1} \quad (2)$$

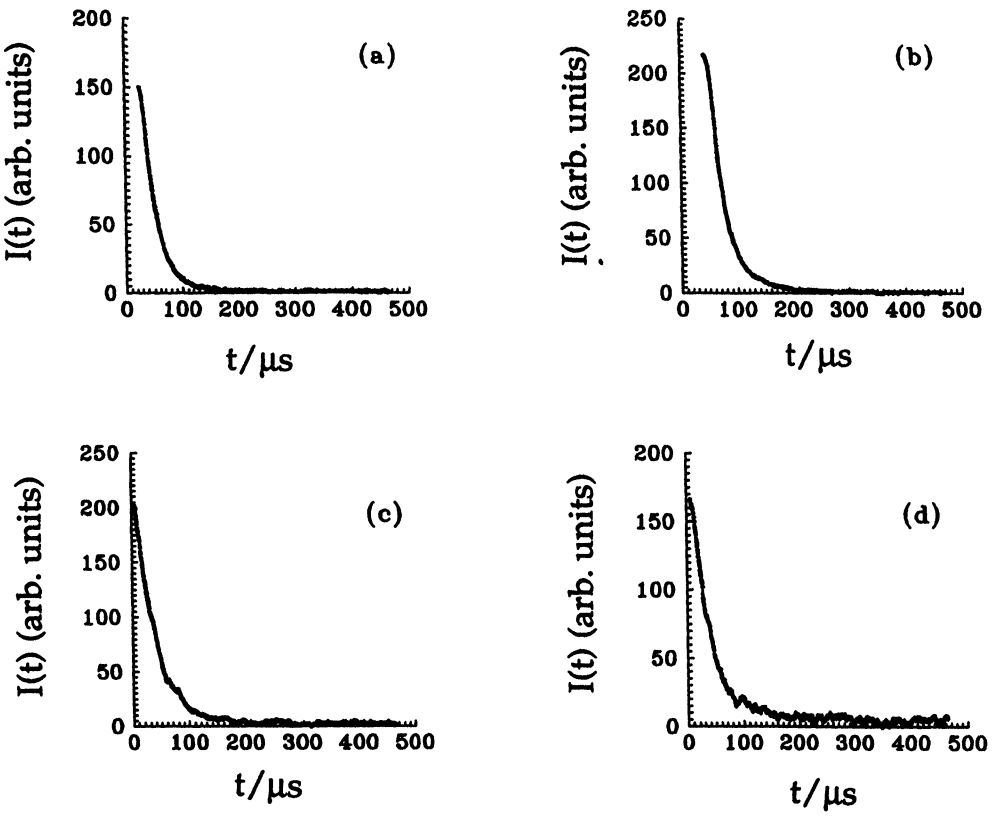

Figure 6 Examples of the digitized output indicating the exponential decay profiles for the time-resolved molecular chemiluminescence from $SrI(A^2\Pi_{3/2} \rightarrow X^2\Sigma^+)$ ($\lambda = 677$ nm, ($\Delta v = 0$)) following the pulsed dye-laser excitation of strontium vapour at $\lambda = 689.3$ nm ($Sr(5^3P_1) \leftarrow Sr(5^1S_0)$) in the presence of varying concentrations of CF_3I and excess helium buffer gas at elevated temperature. ($T = 840$ K, $p_{\text{Total with He}} = 30$ Torr $- 3.9 \times 10^{17}$ atoms cm^{-3}) $[CF_3I]/10^{16}$ molecules cm^{-3}: (a) 0.95; (b) 1.2; (c) 1.4; (d) 1.8

$$Sr(5^3P_J) + CF_3I \rightarrow SrI(A^2\Pi_{3/2}) + CF_3 \qquad \Delta H = -49.2 \text{ kJ mol}^{-1} \quad (3)$$

$$Sr(5^3P_J) + CF_3I \rightarrow SrI(B^2\Sigma^+) + CF_3 \qquad \Delta H = -42.0 \text{ kJ mol}^{-1} \quad (4)$$

($D_0^0(SrI(X^2\Sigma^+)) \geqslant 2.82$ eV (272.1 kJ mol^{-1} [24]); $D_{298}^0(CF_3I) = 223.8 \pm 2.9$ kJ mol^{-1} [40,41]). Thus, $SrI(A^2\Pi_{1/2}, v' \leqslant 25$, $A^2\Pi_{3/2}$, $v' \leqslant 23$) and $SrI(B^2\Sigma^+$, $v' \leqslant 19$) are energetically accessible initially on collision via the above reactions. $SrI(A^2\Pi_{1/2,3/2})$ (172.5 and 176.4 kJ mol^{-1}, respectively and $SrI(B^2\Sigma^+)$ (183.6 kJ mol^{-1}) can also be generated by electronic energy transfer between $Sr(5^3P_J)$ (177.3kJmol^{-1}) and ground state $SrI(X^2\Sigma^+, v'' = 0)$, the latter two states requiring translational energy, and also via (E-E) transfer from the Boltzmann populations in low vibrational levels of the $X^2\Sigma^+$ ground state.

The first-order decay of $Sr(5^3P_J)$ in the presence of CF_3I is clearly established (Figure 2) and can be expressed as

$$[Sr(5^3P_J)]_t = [Sr(5^3P_J)]_{t=0} \exp(-k'(^3P_J)t) \qquad (v)$$

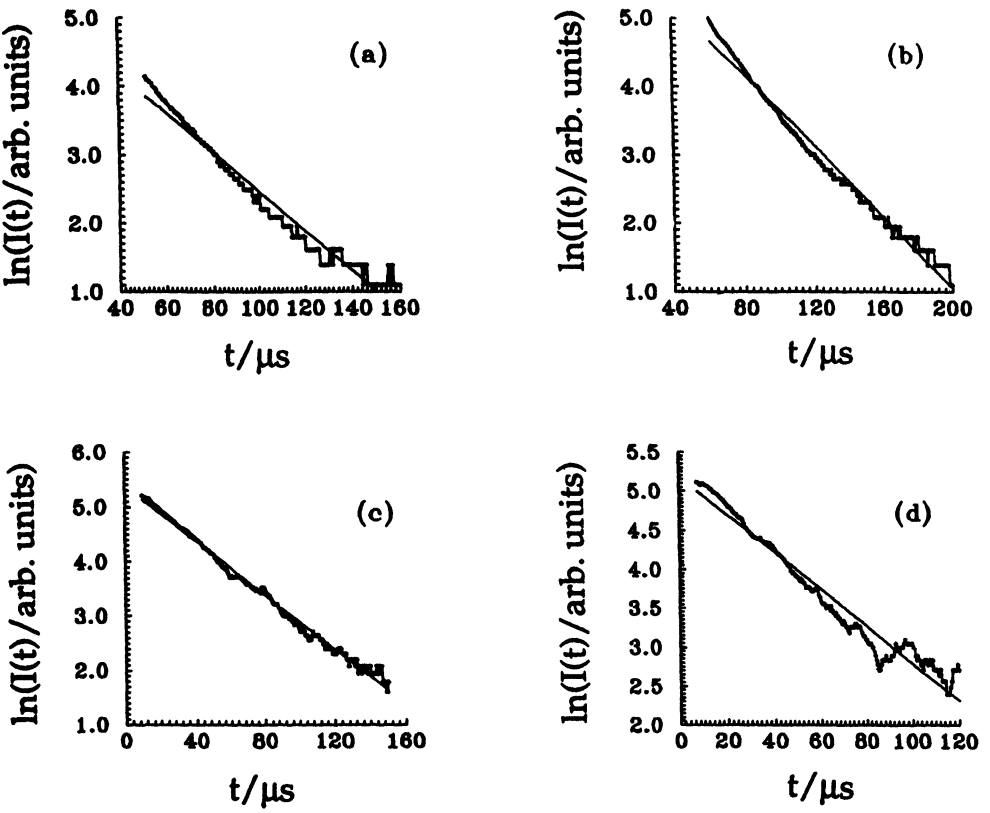

Figure 7 Examples of the computerised fitting of the digitized output indicating the first-order decay for the time-resolved molecular chemiluminescence from $SrI(A^2\Pi_{3/2} \rightarrow X^2\Sigma^+)$ ($\lambda = 677$ nm, ($\Delta v = 0$)) following the pulsed dye-laser excitation of strontium vapour at $\lambda = 689.3$ nm ($Sr(5^3P_1)) \leftarrow Sr(5^1S_0)$) in the presence of varying concentrations of CF_3I and excess helium buffer gas at elevated temperature. ($T = 840K$ $p_{Total\ with\ He} = 30$ Torr $-3\text{-}9 \times 10^{17}$ atoms cm^{-3}) $[CF_3I]/10^{16}$ molecules cm^{-3}: (a) 0.95; (b) 1.2; (c) 1.4; (d) 1.8

where the first-order decay coefficient for $Sr(5^3P_J)$ ($k'(^3P_J)$ is given by equations (iii) and (iv). The mean radiative lifetimes of $SrI(A^2\Pi_{1/2,3/2})$ have been characterised by Dagdigian et al.[42] (τ_e/ns: $A^2\Pi_{1/2}$, 43.3 ± 1.6; $A^2\Pi_{3/2}$, 41.9 ± 1.3) as has that for the $B^2\Sigma^+$ state (τ_e/ns: 46.0 ± 2.0).[42] We may place the concentrations of SrI in the $A^2\Pi_{1/2,3/2}$ and $B^2\Sigma^+$ states in steady state following their direct production by processes (2) – (4) within the time-scales employed in the present investigation. The removal of SrI(A,B) is dominated by emission and is readily given, in the case of $SrI(A_{1/2})$ from $Sr(5^3P_J) + CF_3I$, by

$$I_{em}(A_{1/2} - X) = \Phi k_2[Sr(5^3P_J)]_{t=0} \exp(-k'(^3P_J)t) \qquad \text{(vi)}$$

where Φ represents the combination in individual cases of the effects of light collection, optical sensitivity and electronic amplification of the photoelectric signals. Thus, the first-order coefficients for the decays of the $SrI(A_{1/2}, A_{3/2}, B\text{-}X)$ and $Sr(5^3P_1 \rightarrow 5^1S_0)$ should be equal as indicated in Figures 10 and the time dependencies of the atomic and molecular emission profiles demonstrate the production of the excited molecular states by direct reaction.

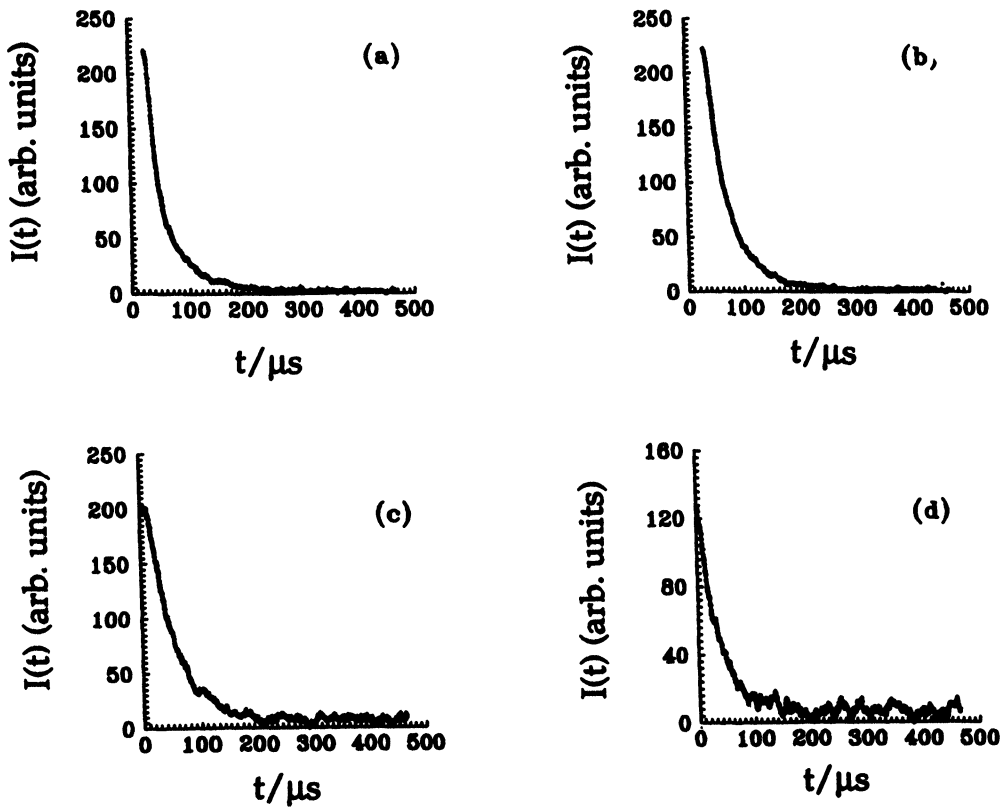

Figure 8 Examples of the digitized output indicating the exponential decay profiles for the time-resolved molecular chemiluminescence from $SrI(B^2\Sigma^+ \rightarrow X^2\Sigma^+)$ ($\lambda = 674$ nm, ($\Delta v = 0$)) following the pulsed dye-laser excitation of strontium vapour at $\lambda = 689.3$ nm ($Sr(5^3P_J) \leftarrow Sr(5^1S_0)$) in the presence of varying concentrations of CF_3I and excess helium buffer gas at elevated temperature. ($T = 840$K, $p_{\text{Total with He}} = 30$ Torr $- 3.9 \times 10^{17}$ atoms cm^{-3}) $[CF_3I]/10^{16}$ molecules cm^{-3}: (a) 0.95; (b) 1.2; (c) 1.4; (d) 1.8

The production of $SrI(A^2\Pi, B^2\Sigma^+)$ by energy transfer from $Sr(5^3P_J)$ to an effectively steady population of $SrI(X^2\Sigma^+)$ in low vibrational levels ($[SrI(X)_{st}]$) resulting from the reaction of $Sr(5^1S_0)+CF_3I$ would add a term of the form $k_R[Sr(5^3P_J)]_{t=0}[SrI(X)]_{st}\exp(-k't)$ to equation (vi) and would not affect the exponential form and the decay coefficients for the $A_{1/2,3/2} - X$ and B-X chemiluminescence emission profiles. Those contributions are difficult to quantify in the present system. As we have stressed in earlier publications on $Sr(5^3P_J)$,[4,5,20,21] this may be contrasted, in this instance, with the relatively large and time-variable concentrations of $SrI(X^2\Sigma^+)$ resulting from the reaction of the high density of $Sr(5^3P_J)$, generated by the pulsed dye-laser excitation process, with CF_3I which would grow approximately with the form $(1 - \exp(-k'(^3P_J)t)$ as a result of the lower reactivity and correspondingly longer lifetime of $SrI(X^2\Sigma^+)$ compared with the short-lived $A^2\Pi$ and $B^2\Sigma^+$ states and also $Sr(5^3P_J)$, itself. An (E – E) transfer mechanism from the Boltzmann population within SrI(X) on this basis would result in molecular chemiluminescence of the form $I_{em}(A,B\text{-}X)$ $\alpha(\exp(-k'(^3P_J)t) - [\exp(-2k'(^3P_J)t))$[4,5,20,21] which would grossly distort the single exponential profiles which is not significantly the case. The present observations on the

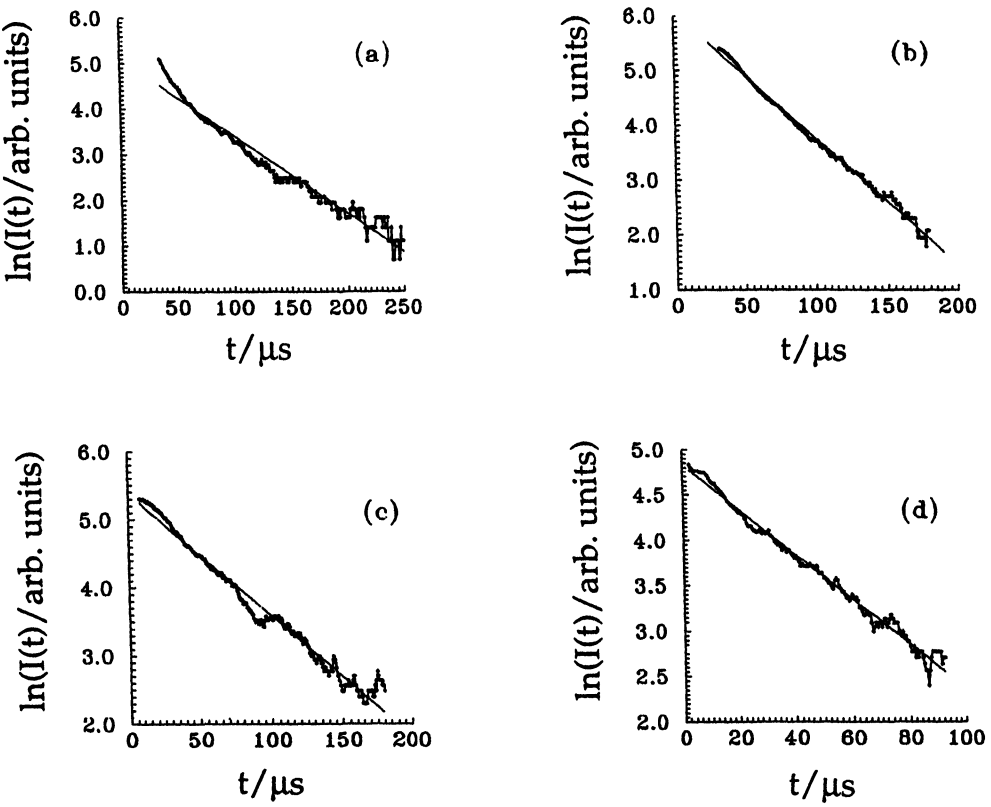

Figure 9 Examples of the computerised fitting of the digitized output indicating the first-order decay for the time-resolved molecular chemiluminescence from $SrI(B^2\Sigma^+ \rightarrow X^2\Sigma^+)$ ($\lambda = 674$ nm, ($\Delta v = 0$)) at long time following the pulsed dye-laser excitation of strontium vapour at $\lambda = 689.3$ nm ($Sr(5^3P_1) \leftarrow Sr(5^1S_0)$) in the presence of varying concentrations of CF_3I and excess helium buffer gas at elevated temperature. ($T = 840$K, $p_{\text{Total with He}} = 30$ Torr $- 3.9 \times 10^{17}$ atoms cm^{-3}) $[CF_3I] / 10^{16}$ molecules cm^{-3}: (a) 0.95; (b) 1.2; (c) 1.4; (d) 1.8

time-dependence of the SrI(A,B-X) chemiluminescence emissions observed here in the time-domain and resulting from direct reaction from $Sr(5^3P_J)$ are in accord with the observation of $SrBr,I(A^2\Pi,B^2\Sigma^+ - X^2\Sigma^+)$ chemiluminescence under molecular beam conditions from the reactions of $Sr(^3P_J)+CH_2Br_2$ and CH_2I_2, respectively,[43] and $SrCl(A,B-X)$ from $Sr(^3P,^1D)+CCl_4$ under single collision conditions.[7,8]

3.2. Branching Ratios

Branching ratios into $SrI(A_{1/2}, A_{3/2}, B)$ from $Sr(5^3P_J)+CF_3I$ may be estimated using measurements of the integrated molecular and atomic intensities derived from the recorded decay profiles and the response of the optical system at different wavelengths and with varying photomultiplier gain, combined with the various rate equations that have been presented. The expression for the atomic emission intensity from $Sr(^3P_1)$ employing equation (v) and noting that emission only arises from this spin-orbit level in the $Sr(^3P_J)$ manifold, is given by

$$I_{(3P)} = \{A_{nm}/F\}\,[Sr(5^3P_J)]_{t=0}\exp\{-k'(^3P_J)t\} \qquad \text{(vii)}$$

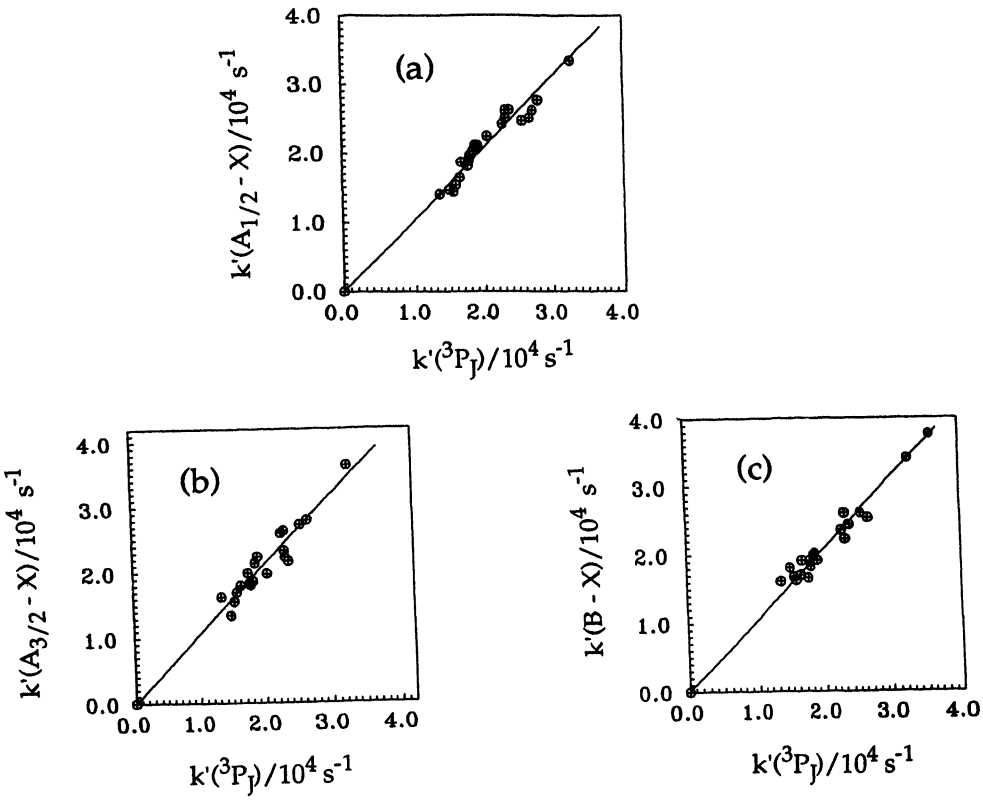

Figure 10 Comparison of the first-order rate coefficients derived from the intensity profiles for the (a) $SrI(A^2\Pi_{1/2}-X^2\Sigma^+)$ ($\Delta v=0$, $\lambda=694$ nm), (b) $SrI(A^2\Pi_{3/2}-X^2\Sigma^+)$ ($\Delta v=0$, $\lambda=677$ nm) and (c) $SrI(B^2\Sigma^+\rightarrow X^2\Sigma^+)$ ($\Delta v=0$, $\lambda=674$ nm) molecular chemiluminescence emissions ($k'(A_{1/2}-X)$, $k'(A_{3/2}-X)$) and $k'(B - X)$, respectively) with those from the atomic emission profiles for the decay of $Sr(5^3P_1)$ at $\lambda=689.3$ nm ($Sr(5^3P_1)\rightarrow Sr(5^1S_0)$) ($k'(^3P)$) following the pulsed dye-laser generation of $Sr(5^3P_J)$ at the resonance wavelength ($Sr(5s5p(^3P_1))\leftarrow Sr(5s^2(^1S_0))$) in the presence of varying concentrations of CF_3I and excess helium buffer gas at $T=840$ K . Slope: (a) 1.04; (b) 1.06; (c) 1.04

where $A_{nm}=1/\tau_e$ for $Sr(5^3P_1)$, and F and $k'(^3P_j)$ (k') have been defined hitherto. The integrated intensity is thus given by

$$I(Sr^3P_J)=A_{nm}[Sr(5^3P_J]_{t=0}/k'(^3P_J)F \qquad \text{(viii)}$$

Placing $[SrI(A^2\Pi_{1/2})]$ resulting from reaction with CF_3I in equation (2) in steady state where its production is balanced by rapid spontaneous emission, the emission intensity from $SrI(A_{1/2}-X)$ is given by

$$I_{A_{1/2}}=k_{2(A_{1/2})}f[CF_3I][Sr(5^3P_J]_{t=0}\exp\{-k'(^3P_J)t\} \qquad \text{(ix)}$$

employing equation (vi), where f is the fraction of the initial $[CF_3I]$ entering the excitation zone which is taken, within significant experimental error, to be constant in this estimation (Figure 3). $k_{2(A_{1/2})}$ is the rate constants for the production of $SrI(A^2\Pi_{1/2})$ via equation (2). Hence, from the foregoing kinetic analysis, the result for the ratio of the integrated molecular intensity for $SrI(A_{1/2}-X)$, for example, to that of the $^3P_1-{}^1S_0$ atomic emission, is given by the ratio of the integrated form of equation (ix) and of

equation (viii), namely,

$$I\{SrI(A_{1/2}-X)\}/I\,(Sr^3P_1) = k_{2(A_{1/2})}F\tau_e f[CF_3I] \qquad (x)$$

Thus, it may be seen that the ratio of the slopes of the plots of (a) $I\{SrI(A_{1/2}-X)\}/I(Sr^3P_J)$ versus $[CF_3I]$ (Figure 11(a)), and (b), $k'(^3P_J)$ versus $[CF_3I]$ (Figure 3), yields the branching ratio for $SrI(A^2\Pi_{1/2})$, namely, $k_2(A_{1/2})/k_R$. The relevant plots for component (a) for $SrI(A_{3/2},B)$ are also given in Figure 11. The branching ratios into the excited states obtained in this investigation are thus found to be as follows: $A_{1/2}$, 1.2×10^{-2}; $A_{3/2}$, 6.7×10^{-3}; B, 5.1×10^{-3}. This yield of $\Sigma(SrI(A_{1/2}, A_{3/2}, B^2\Sigma^+) = 2.4\times10^{-2}$ and can be compared with the similar result for $Sr(5^3P_J)+CH_3I$[5] and other halogen abstraction reactions of this optically metastable atom.[4,5,26,27] It may also be compared with analogous molecular beam data where only the total yield into analogous excited states are reported and found to be ca. 1.5×10^{-3} and 9.5×10^{-3} for $Ca(4^3P_J)+CH_2Br_2$ and $Ca(4^3P_J)+CH_3Cl$ (CaBr and CaCl $A^2\Pi$ and $B^2\Sigma^+$ states), respectively.[22] Further, assuming that removal of $Sr(5^3P_J)+CF_3I$ proceeds entirely by I-atom abstraction into $SrI(A_{1/2}, A_{3/2}, B, X)$, higher states of SrI not being energetically

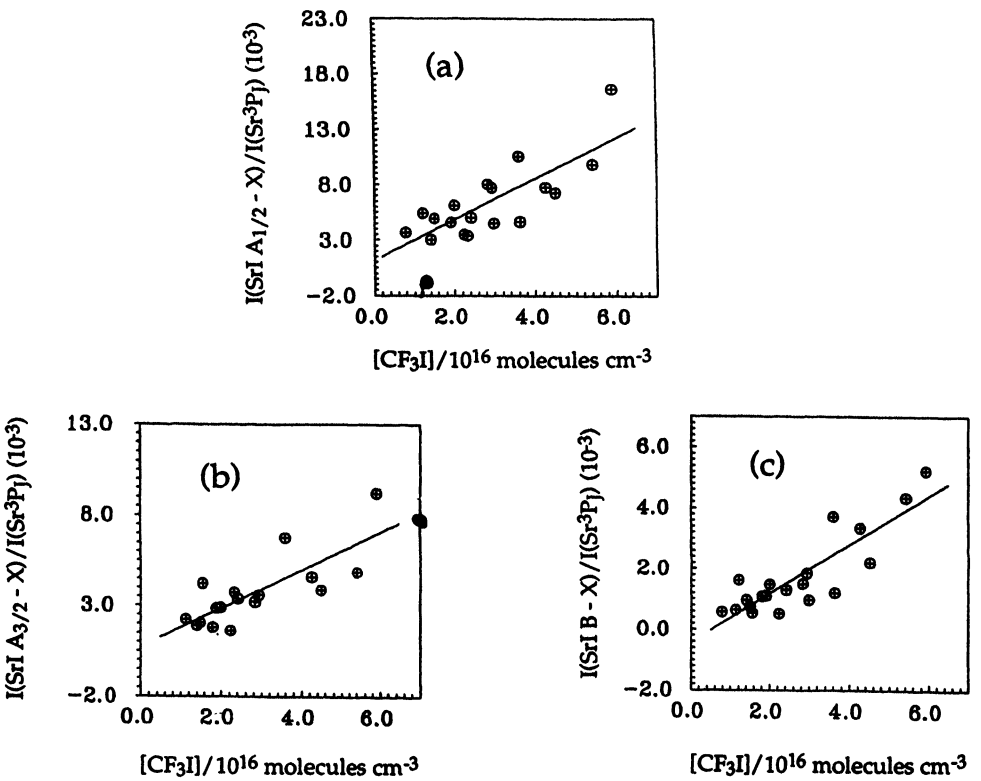

Figure 11 Variations of the integrated intensity ratios of the molecular chemiluminescence emissions to the atomic fluorescence emission $Sr(5^3P_1 \rightarrow 5^1S_0)$ ($\lambda = 689.3$ nm) for (a) $SrI(A^2\Pi_{1/2} \rightarrow X^2\Sigma^+$, $\Delta v = 0$, $\lambda = 694$ nm), (b) $SrI(A^2\Pi_{3/2} \rightarrow X^2\Sigma^+$, $\Delta v = 0$, $\lambda = 677$ nm) and (c) $SrI(B^2\Sigma^+ \rightarrow X^2\Sigma^+$, $\Delta v = 0$, $\lambda = 674$ nm) as a function of the concentration of CF_3I following the pulsed dye-laser excitation of strontium vapour at the resonance wavelength ($\lambda = 689.3$ nm) and in the presence of excess helium buffer gas at elevated temperature. ($T = 840$ K)

accessible, this, in turn yields an upper limit for the branching ratio into $SrI(X^2\Sigma^+)$ of ca. 98% in view of the possible role of physical quenching of $Sr(5^3P_J)$ into $Sr(5^1S_0)$ by CF_3I. The appropriate data for $Sr(5^3P_J)$ from molecular beams are not available, to the best of our knowledge. It is concluded from the quality of Figure 3 and particularly Figure 11 that the results for the relative branching ratios for the $SrI(A_{1/2},A_{3/2},B)$ states are more accurate than the absolute values. Nevertheless, they do constitute, to the best of our knowledge, the first absolute data of this kind into these specific electronic states. As with the molecular beam data for $Ca(4^3P_J)$,[22] they demonstrate the dominance of ground state production.

Finally, we may summarise branching ratio data into the exothermically accessible $A^2\Pi_{1/2}$, $A^2\Pi_{3/2}$ and $B^2\Sigma^+$ states of the strontium halides (SrX*) resulting from the reaction of $Sr(5^3P_J)$ with the molecules CF_3I, CH_3I, CH_3F, CH_2Cl_2 and CH_2Br_2.[4,5,20,21] These have recently become accessible from measurements in the time-domain following the development in data capture and analysis methods, and sensitivity calibration techniques described in this paper and, in our view, constitutes a novel contribution to this general area of atomic collisions. Data reported for branching ratios into the $SrX(X^2\Sigma^+)$ ground states in general can only be regarded as upper limits for reasons presented in the specific case for $Sr(5^3P_J)+CF_3I$ given here. The results are summarised in Table 1. The compilation does not include data for branching ratios into specific electronic states for reactions of $Sr(5^3P_J)+CH_3Cl$, CF_3Cl, CH_3Br and CF_3Br as those investigations employed the earlier boxcar integration methods and the optical calibration method was not available at that time.[2,3] A correlation can be seen between the measured branching ratios across the limited energy ranges of the $A^2\Pi_{1/2,3/2}$ and $B^2\Sigma^+$ states and the energy of the states, namely, the semi-logarithmic variation presented in Figure 12. The inverse in the slope in Figure 12 for the data describing branching ratios into $SrI(A_{1/2},A_{3/2},B)$ from $Sr(5^3P_J)+CF_3I$ corresponds to a temperature of ca. 700K and similar results are seen for the other systems investigated. An identical slope was obtained for the branching ratios into $SrI(A_{1/2},A_{3/2},B)$ from $Sr(5^3P_J)+CH_3I$ (Figure 12),[5] notwithstanding the greater branching ratios into $SrI(A_{1/2},A_{3/2},B)$ observed here for $Sr(5^3P_J)+CF_3I$. Strong accuracy is not claimed for these slopes in view of the limitations necessarily encountered in the measurements of integrated intensities but one may note that the effective temperatures (via k_BT,/hc, cm^{-1}) are similar and close to the ambient temperatures that have been employed (Table 1). This type of relationship demonstrated in Figure 12 is common to a range of energy transfer processes in gases. This approximate dependence of the branching

Table 1 Branching ratios into $SrX^*(A^2\Pi_{1/2}, A^2\Pi_{3/2}, B^2\Sigma^+)$ from the halogen atom abstraction reactions of $Sr(5^3P_J)$ with halogenated methanes determined by time-resolved measurements of atomic fluorescence (5^3P_1-5^1S_0) and molecular chemiluminescence $SrX^*(A_{1/2},A_{3/2},B\text{-}X)$ following pulsed dye-laser excitation.

Halogenated Methane	$A_{1/2}$	$A_{3/2}$	B	$\Sigma\,(A_{1/2}+A_{3/2}+B)$	T/K
CF_3I*	1.2×10^{-2}	6.7×10^{-3}	5.1×10^{-3}	2.4×10^{-2}	840
CH_3I[5]	6.9×10^{-3}	3.5×10^{-3}	3.0×10^{-3}	1.3×10^{-2}	840
CH_3F[4]	6.4×10^{-3}	1.5×10^{-3}	1.1×10^{-4}	8.0×10^{-3}	850
CH_2Cl_2[20]	3.0×10^{-3}	1.7×10^{-3}	4.4×10^{-4}	5.1×10^{-3}	850
CH_2Br_2[21]	5.4×10^{-3}	3.7×10^{-3}	1.3×10^{-3}	1.0×10^{-2}	840

[*] This work

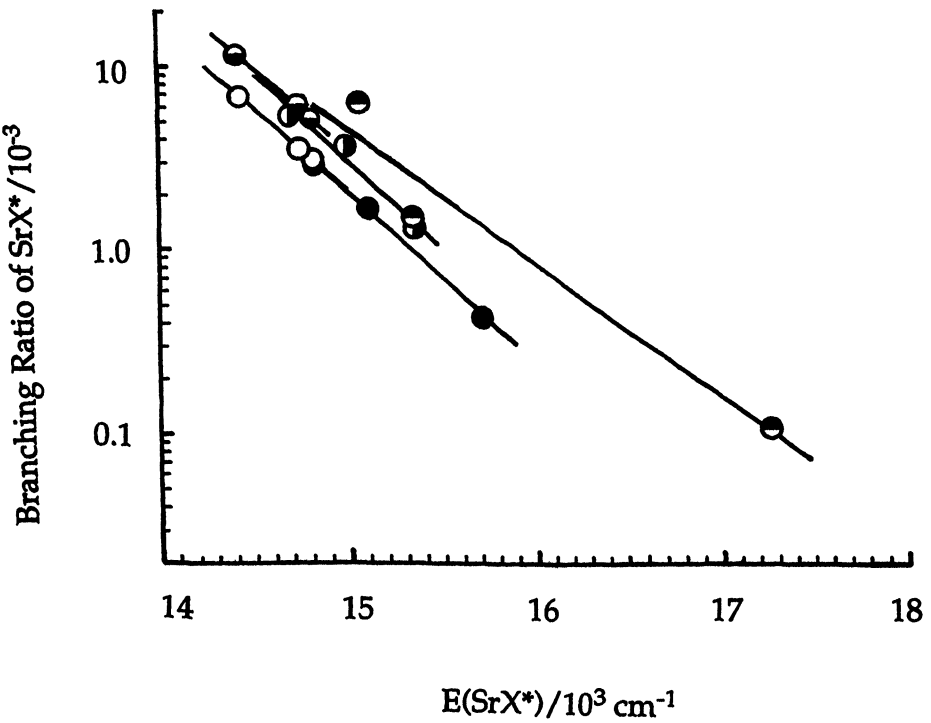

Figure 12 Variation of the branching ratio into electronically excited strontium halides, SrX*, (X = F, Cl, Br, I; SrX* $A^2\Pi_{1/2}$, $A^2\Pi_{3/2}$ $B^2\Sigma^+$) observed by time-resolved molecular chemiluminescence following halogen abstraction reactions by $Sr(5^3P_J)$ generated by pulsed dye-laser excitation of strontium vapour at elevated temperatures in the presence of various halogenated methanes, as a function of the electronic energy of the state, E(SrX*).◒ CF_3I (this work); ○ CH_3I;[5] ◓ CH_3F;[4] ● CH_2Cl_2;[20] ◑ CH_2Br_2[21]

ratio with the Boltzmann form, albeit over a limited energy range, corresponding roughly with the ambient temperature, indicates the absence of a strong propensity restriction.This could be expected on the basis of (J,Ω) coupling[44] where, in this case, all the spin-orbit states within the reacting Boltzmannised $Sr(5^3P_J)$ manifold would have to be considered separately together with the Hund's case (c) components of product states. Many surfaces would be involved with a number of surface crossings. This is in some contrast with molecular beam measurements on $Sr(5^3P_{0,1,2})$ where the behaviour of individual spin-orbit components can be investigated by optical pumping methods.[9] Finally, we may also note that the observed dependence of the branching ratios with the energy of the state also indicates the role of 'late barriers' in the transition states for all cases of halogen abstraction involving $Sr(5^3P_J)$ investigated in the time-domain so far.

Acknowledgements

We thank the Cambridge Overseas Scholarship Trustees for a Research Studentship held by J.L. during the tenure of which this work was carried out. J.L. also thanks the O.R.S. for an award. We also thank the E.P.S.R.C. of Great Britain for a Research Studentship held by one of us (S.A.) and for the initial purchase of the laser system.

F.C., M.N.S.R. and D.H. are grateful to the British Council and the Acciones Integradas (Spain) for a travel grant which made this collaboration possible. Finally, we are also indebted to Dr. George Jones of the DRA (Fort Halstead) for encouragement and helpful discussions.

References

1. C. E. Moore, Ed., "Atomic Energy Levels", Nat.Bur.Stand.Ref. Data Ser., Vol. Parts I–III, (U.S. Government Printing Office, Washington, D.C., 1971).
2. M. N. Sanchez Rayo, F. Castaño, M. T. Martinez, J. W. Adams, S. A. Carl, D. Husain and J. Schifino, J. Chem. Soc. Faraday Trans. **89**,1645 (1993).
3. F. Castaño, M. N. Sanchez Rayo, R. Pereira, J. W. Adams, D. Husain and J. Schifino, J. Photochem. Photobiol., **A 83**, 79 (1994).
4. S. Antrobus, S. A. Carl, D. Husain, J. Lei, F. Castaño and M. N. Sanchez Rayo, Ber. Bunsen. Ges. Phys. Chem., **99**, 127 (1995).
5. S. Antrobus, D. Husain, Jie Lei, F. Castaño and M. N. Sanchez Rayo, Z. Phys. Chem., (1995) submitted. (paper no. 1006).
6. T. Kiang, R. C. Estler and R. N. Zare, J. Chem. Phys., **70**, 5925 (1979).
7. U. Brinkmann, V. H. Schmidt and H. Telle, Chem. Phys. Lett., **73**, 530 (1980).
8. U. Brinkmann, V. H. Schmidt and H. Telle, Chem. Phys., **64**,19 (1982).
9. P. J. Dagdigian and M. L. Campbell, Chem. Rev., **87**,1(1987).
10. D. Husain and G. Roberts, in 'Bimolecular Collisions: Advances in Gas Phase Photochemistry and Kinetics', Ed. M. N. R. Ashfold and J. E. Baggott, The Royal Society of Chemistry, London, 1989, Chapter 6, p. 263.
11. W. H. Breckenridge and H. Umemoto, Adv. Chem. Phys., **50**, 325 (1982).
12. W. H. Breckenridge, in 'Reactions of Small Transient Species: Kinetics and Energetics', Ed., A. Fontijn and M. A. A. Clyne, Academic Press, London, 1983, Chapter 4, p. 157.
13. D. Husain, J. Chem. Soc. Faraday Trans. 2, **85**, 85 (1989).
14. R. W. Solarz and S. A. Johnson, J. Chem. Phys., **70**, 3593 (1979).
15. R. W. Solarz, S. A. Johnson and R. K. Preston, Chem. Phys. Lett., **57**, 514 (1978).
16. F. Beitia, F. Castaño, M. N. Sanchez Rayo, S. A. Carl, and D. Husain, J. Photochem. Photobiol., Chem., **A 62**,1(1991).
17. F. Beitia, F. Castaño, M. N. Sanchez Rayo, S. A. Carl, D. Husain and L. Santos, J. Chem. Soc. Faraday Trans. **87**, 2413 (1991).
18. F. Beitia, F. Castaño, M. N. Sanchez Rayo, S. A. Carl, D. Husain and L. Santos, Z. Phys. Chem., **N. F. 171**,137 (1991).
19. F. Basterrechea, F. Beitia, F. Castaño, M. N. Sanchesz Rayo, S. A. Carl, and D. Husain, Ber. Bunsen. Ges. Phys. Chem., **95**,1615 (1991).
20. S. Antrobus, D. Husain, Jie Lei, F. Castaño and M. N. Sanchez Rayo, Int. J. Chem. Kinet., 1994, in press (paper no. 113199).
21. S. Antrobus, D. Husain, Jie Lei, F. Castaño and M. N. Sanchez Rayo, J. Chem. Res., (5) 84–85 (1995), (M) 0601–0629 (1995).
22. N. Furio, M. L. Campbell and P. J. Dagdigian, J. Chem. Phys., **84**, 4332 (1986).
23. CRC Handbook of Physics and Chemistry, 75th. Edition, Eds. D. R. Lide and H. P. R. Frederikse (CRC Press, Boca Raton, Florida, U.S.A., 1994) p. 4–124.
24. K. P. Huber and G. Herzberg, *Molecular Spectra and Molecular Structure. IV. Constants of Diatomic Molecules* (Van Nostrand Reinhold, New York, 1979).
25. B. Rosen, Ed., *Spectroscopic Data Relative to Diatomic Molecules* (Pergamon, New York, 1970).
26. J. O. Schröder, C. Nitsch and W. E. Ernst, J. Molec. Spectr., **132**,166 (1988).
27. W. E. Ernst, J. O. Schröder and B. Zeller, J. Molec. Spectr., **135**, 61 (1989).
28. E. M. I. Catalogue (E.M.I. Industrial Publications, 1979).
29. D. Husain and J. Schifino, J. Chem. Soc. Faraday Trans 2, **80**, 321(1984).
30. D. Husain and G. Roberts, Chem. Phys., **127**, 203 (1988).
31. D. Husain and J. Schifino, J. Chem. Soc. Faraday Trans. 2, **80**, 647 (1984).
32. C. H. Corliss and W. R. Bozman, *Experimental Transition Probabilities for Spectral Lines of Seventy Elements*, Nat.But.Stand. Monograph 53 (U.S. Government Printing Office, Washington, D.C., 1962) pps. 388–389.
33. J. F. Kelley, M. Harris and A. Gallagher, Phys. Rev. A., **37**, 2354 (1988).
34. T. J. McIlrath and J. L. Carlsten, J. Phys. B., **6**, 697 (1973).

35. F. Beitia, F. Castaño, M. N. Sanchez Rayo and D. Husain, Chem. Phys., **166**, 275 (1992).
36. R. S. Clay and D. Husain, J. Photochem. Photobiol., Chem., **A 56**,139 (1991).
37. R. S. Clay and D. Husain, Comb. and Flame, **86**, 371 (1991).
38. R. P. Tuckett, (1992) private communication..
39. W. E. Ernst (1993) private communication.
40. CRA Handbook of Physics and Chemistry, 75th. Edition, Eds. D. R. Lide and H. P. R. Frederikse (CRC Press, Boca Raton, Florida, U.S.A., 1994) p. **9**–66.
41. S. I. Ahonklai and E. Whittle, Int. J. Chem. Kinetics, **16**, 543 (1984).
42. P. J. Dagdigian, H. Cruse and R. N. Zare, J. Chem. Phys., **60**, 2330 (1974).
43. M. I. Campbell and P. J. Dagdigian, J. Amer. Chem. Soc., **108**, 4701(1986).
44. D. Husain, Ber,Bunsen. Ges. Phys. chem., **81**,168 (1977).